Strain compensation in InGaN-based multiple quantum wells using AlGaN interlayers

Syed Ahmed Al Muyeed, Wei Sun, Xiongliang Wei, Renbo Song, Daniel D. Koleske, Nelson Tansu, and Jonathan J. Wierer

Citation: AIP Advances **7**, 105312 (2017); doi: 10.1063/1.5000519
View online: http://dx.doi.org/10.1063/1.5000519
View Table of Contents: http://aip.scitation.org/toc/adv/7/10
Published by the American Institute of Physics

AIP ADVANCES **7**, 105312 (2017)

Strain compensation in InGaN-based multiple quantum wells using AlGaN interlayers

Syed Ahmed Al Muyeed,[1,a] Wei Sun,[1] Xiongliang Wei,[1] Renbo Song,[1] Daniel D. Koleske,[2] Nelson Tansu,[1,b] and Jonathan J. Wierer, Jr.[1,c]
[1]*Center for Photonics and Nanoelectronics and Electrical and Computer Engineering, Lehigh University, Bethlehem, PA 18015, USA*
[2]*Sandia National Laboratories, Albuquerque, NM 87185, USA*

(Received 16 August 2017; accepted 6 October 2017; published online 16 October 2017)

Data are presented on strain compensation in InGaN-based multiple quantum wells (MQW) using AlGaN interlayers (ILs). The MQWs consist of five periods of $In_xGa_{1-x}N/Al_yGa_{1-y}N/GaN$ emitting in the green ($\lambda \sim 535$ nm $\pm$ 15 nm), and the $Al_yGa_{1-y}N$ IL has an Al composition of $y = 0.42$. The IL is varied from 0 - 2.1 nm, and the relaxation of the MQW with respect to the GaN template layer varies with IL thickness as determined by reciprocal space mapping about the $(20\bar{2}5)$ reflection. The minimum in the relaxation occurs at an interlayer thickness of 1 nm, and the MQW is nearly pseudomorphic to GaN. Both thinner and thicker ILs display increased relaxation. Photoluminescence data shows enhanced spectral intensity and narrower full width at half maximum for the MQW with 1 nm thick ILs, which is a product of pseudomorphic layers with lower defect density and non-radiative recombination.
https://doi.org/10.1063/1.5000519

III-nitride violet-blue light-emitting diodes (LEDs) are some of the highest efficiency light sources ever created,[1–5] and use InGaN-based multiple quantum wells (MQWs) as active layers. These InGaN-based MQWs can also emit at longer wavelengths (green-red) when the indium concentration is increased ($x \geq 0.20$)[6] to cover the whole visible range and produce white light. However, it has proven difficult to realize the same high radiative efficiency at these longer wavelengths. This lack of high efficiency at green to red wavelengths is known as the "green gap".[7,8] There are several causes behind this decrease in efficiency at longer wavelengths that include — high lattice mismatch strain between the InGaN quantum wells (QWs) and GaN barriers that results in defect formation and non-radiative recombination;[9–11] a low InGaN growth temperature used to incorporate indium which results in impurities, point defects, and V-type defects;[12–16] and finally, polarization-induced charge separation effect that decreases electron and hole wavefunction overlap.[17–19] All these effects result in increased defects and non-radiative recombination, decreased spontaneous emission rate, and an overall lower efficiency.

It has been shown that using thin AlGaN interlayers (ILs) grown on top of InGaN QWs results in a drastic improvement in the external quantum efficiency of LEDs at green-red wavelengths.[20–22] Using AlGaN ILs is not intuitive, and there are several possible reasons for the observed improvement. Scanning transmission electron microscope (STEM) images show that AlGaN ILs "cap" the InGaN QWs, producing smoother and more abrupt heterointerfaces compared to InGaN/GaN heterointerfaces.[20,23] This suggests the AlGaN IL reduces out-diffusion of indium from the QWs, and this notion is confirmed with higher indium concentration QWs with AlGaN ILs.[23,24] Additionally, ILs enable higher temperature growth of the GaN barriers, and this higher temperature growth anneals the

[a]Email: sya216@lehigh.edu
[b]Email: tansu@lehigh.edu
[c]Email: jwierer@lehigh.edu

QW and the ILs. This annealing improves the material quality and reduces impurity incorporation.[23,25] This is contrary to standard InGaN/GaN MQWs where higher growth temperatures of the barriers are avoided. All these effects increase the spontaneous emission rate, and thus the external quantum efficiency. Finally, introducing an AlGaN IL increases the piezoelectric polarization induced electric field, which further tilts the energy bands and reduces energy transitions. Although this will decrease wavefunction overlap, it does produce longer wavelengths without increasing the indium concentration in the QWs.

Another possible effect that has recently been discussed in interlayer MQWs is the role of strain compensation.[26,27] InGaN QWs grown on GaN are compressively strained with respect to GaN, whereas, AlGaN ILs are under tensile strain. Therefore, AlGaN ILs can act as a strain compensating layer for InGaN QWs and force pseudomorphic growth of the entire MQW stack with significantly reduced strain relaxation. Such effects have been observed in other III-V compound semiconductors.[28,29] In previous work in III-nitrides, it is assumed that the interlayer provides full strain compensation[26] and pseudomorphic growth; however, it has yet to be verified and quantified. Producing pseudomorphic MQWs is desirable, because it will prevent defect formation and result to a pathway toward higher efficiency.

In this letter, strain compensation is demonstrated using AlGaN ILs in InGaN-based MQWs emitting in the green spectral regime. Reciprocal space maps about the $(20\bar{2}5)$ reflection are used to determine the degree of relaxation of the MQWs. At an Al composition (y) of y = 0.42 and thickness of 1 nm for the $Al_yGa_{1-y}N$ interlayer, the MQW stack is nearly pseudomorphic with a relaxation of only ~0.07%. The Al composition in the interlayer is chosen to nearly match previous reports.[20,23] Additionally, improved photoluminescence efficiency is observed, which is consistent with previous reports[23] of higher external quantum efficiencies due to lower defect formation and higher radiative efficiency.

The MQW structures are grown by metal-organic chemical vapor deposition (MOCVD) in a vertical-flow Veeco P-75 reactor. The sources consist of triethylgallium (TEGa), trimethylindium (TMIn), trimethylaluminum (TMAl), and ammonia (NH_3). The interlayer MQWs are formed on unintentionally-doped (uid) GaN templates, grown on *c*-plane sapphire substrates at a pressure of 500 Torr and a temperature of ~ 1050 ^{0}C. The MQW is grown at a pressure of 200 Torr, and consists of an initial GaN barrier layer followed by five periods of an InGaN QW, an AlGaN IL and a GaN barrier stack as shown in Figure 1. The InGaN QWs and AlGaN ILs are grown at a fixed temperature of ~ 730 ^{0}C based on the pyrometer temperature reading. To grow the GaN barrier, the temperature is increased to ~ 905 ^{0}C. This is followed by a decrease in temperature to start the growth of the next InGaN QW. Four different interlayer MQWs are grown, all the same except for the IL thickness which is varied from 0.4 nm - 2.1 nm. For comparison, another 5 period InGaN/GaN MQW structure without an AlGaN IL is grown under a slightly different growth sequence. For this structure, the QWs are again grown at 730 ^{0}C, but the GaN barrier is grown at a lower temperature of 830 ^{0}C. This lower barrier temperature is necessary in order to prevent out diffusion of indium from the InGaN QWs and maintain similar indium concentration in all the MQW structures for better comparison.

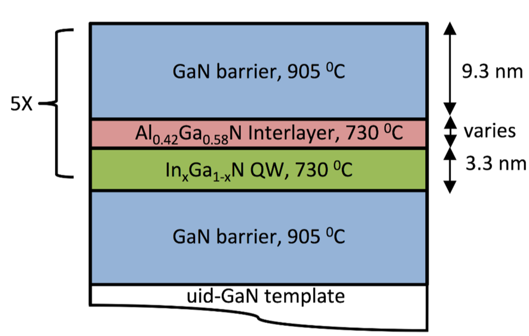

FIG. 1. Cross-sectional schematic of the multiple quantum well structure, consisting of 5 periods of an InGaN quantum well (QW), AlGaN interlayer, and GaN barrier. The structure is grown on an unintentionally doped (uid) GaN layer, and the growth temperatures and layer thicknesses are indicated for each layer.

The thickness and composition of the QWs, ILs, and barriers are determined using a combination of X-ray diffraction (XRD) ω-2Θ scans and optical reflectance measurements on the MQW samples and single layer test structures. The thicknesses are given in nm instead of monolayers, because in the XRD measurements there is averaging that occurs over large areas. To determine the relaxation of the MQWs, reciprocal space mapping (RSM) of ($20\bar{2}5$) reflection are performed using a Panalytical PIXcel-3D detector. The separations in the GaN peak and the 0^{th} peak of the MQWs fringe peaks provide the relaxation percentage of the interlayer MQWs. The percentage of strain relaxation of the MQW stack with respect to GaN is calculated using

$$strain\_relaxation = \frac{\Delta Q_x \; of \; MQWs \; 0^{th} \; peak}{\Delta Q_x \; of \; fully \; relaxed \; In_xGa_{1-x}N}, \tag{1}$$

where, ΔQ_x are differences between the lateral positions of the MQW superlattice peak and GaN substrate peak. Photoluminescence is performed using a laser diode emitting at 405 nm with a power of ~100 mW and an approximated spot size diameter of 0.5 mm.

The $Al_yGa_{1-y}N$ interlayers have an Al composition of y=0.42, and thicknesses of 0.4 nm, 1 nm, 1.7 nm, and 2.1 nm. The GaN barrier is 9.3 nm thick for the interlayer MQW, and is slightly thicker at 9.5 nm for the structure without the IL. The InGaN QWs are 3.3 nm thick for all samples, but the indium concentration varies with IL thickness as shown in Figure 2. Although a lower growth temperature is used to grow the barrier for the standard $In_xGa_{1-x}N$/GaN MQW, the indium concentration is lower than the interlayer MQWs at x = 0.19. The interlayer MQW with a 0.4 nm thick IL has a slightly higher indium concentration in the $In_xGa_{1-x}N$ QW at x = 0.195. At IL thicknesses of 1 nm or greater the indium concentration is constant at x = 0.205. This increase in indium concentration with interlayer thickness is an indication that the AlGaN IL helps prevent out-diffusion (caps) of indium from the InGaN QW.[30] Therefore, the IL enables higher indium concentration in the QW at higher growth temperatures compared to MQWs without the IL. Previous work has shown this higher temperature growth of the QW is desirable, because it results in higher radiative efficiency QWs.[21,23]

Fig 3(a) shows the RSM of the MQW structure without the IL. The GaN is indicated by the most intense peak, and the MQWs result in the fringe peaks that span vertically above and below the GaN peak. There is a very small but detectable difference between the lateral positions of the MQW fringe peaks and the GaN substrate peak at this scale. The difference in lateral positions of the GaN peak and the fringe peaks of the MQWs corresponds to strain relaxation of the MQWs.[31]

In order to clearly discern the differences in the peaks, a closer view of the RSM of the MQW without the IL is shown in Fig 3(b). Here only the GaN peak and the 0^{th} peak of the MQW are visible. For the MQW without the IL, the lateral difference in peaks is ΔQ_x=64 x 10^{-6} reciprocal lattice units (rlu), towards the direction of InGaN relaxation. With the introduction of a 0.4 nm thick

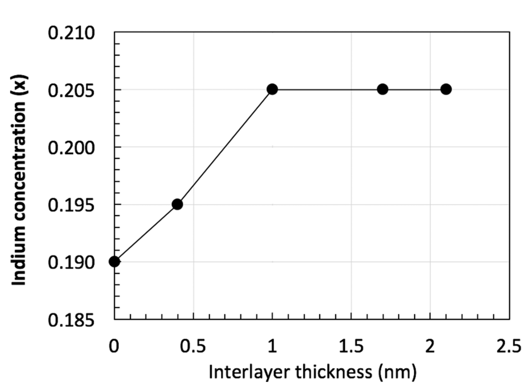

FIG. 2. Indium concentration (x) of the $In_xGa_{1-x}N$ quantum wells versus interlayer thickness measured by X-ray diffraction, Omega-2theta scans of (0002) reflection. The IL caps the InGaN QW, increasing the indium composition. For the data corresponding to IL thickness of 0 nm, the barrier is grown at a temperature of 830^0 C. For the other IL thicknesses, the barriers are grown at a temperature of 905^0 C.

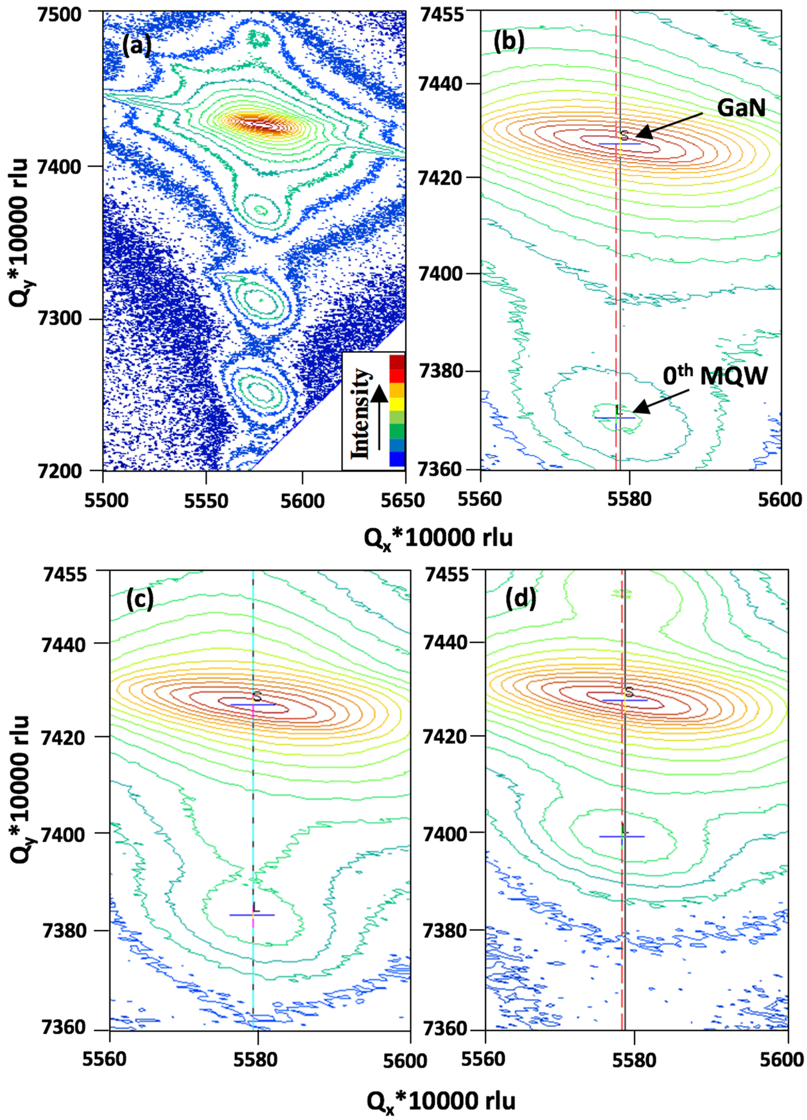

FIG. 3. Reciprocal space map of the $(20\bar{2}5)$ reflection of a) an InGaN/AlGaN/GaN multiple quantum well (MQW) structure with a 0 nm thick AlGaN interlayer. Reciprocal space maps, showing only the GaN and 0^{th} MQW peak, of the MQW structures with b) 0 nm, c) 1 nm, and d) 2.1 nm thick AlGaN interlayers. Solid lines and broken lines indicate positions of the GaN template peaks and the MQW fringe peaks, respectively.

IL, the separation of the peaks become smaller and is measured to be ΔQ_x=48 x 10^{-6} rlu. This shows the tensile strained IL is beginning to compensate for the compressive strain in the QW. Then as the IL thickness is increased to 1 nm, the lateral separation between the peaks becomes smaller and is measured at ΔQ_x=8 x 10^{-6} rlu (Fig 3(c)). This represents the lowest relaxation in the study, but is it is possible that the minimum relaxation is slightly off from 1 nm. As the IL is increased beyond 1 nm, the separation between the position of the GaN and MQW peaks increases. For the MQWs with 1.7 nm thick and 2.1 nm thick ILs, the differences between the MQW peaks and GaN peak are ΔQ_x=36 x 10^{-6} rlu, and ΔQ_x=43 x 10^{-6} rlu (Fig 3(d)), respectively. These shifts are again in the direction of InGaN relaxation.

The peak separations indicated here are measured from the positions of GaN peak and the MQWs 0^{th} fringe peak. In general, the higher order peaks form along the same vertical line as the 0^{th} peak.[31] However, it should be noted that for the 2.1 nm thick IL the higher order peaks begin to break this vertical linear symmetry. The MQW peaks below the GaN peak are shifted slightly in the direction of

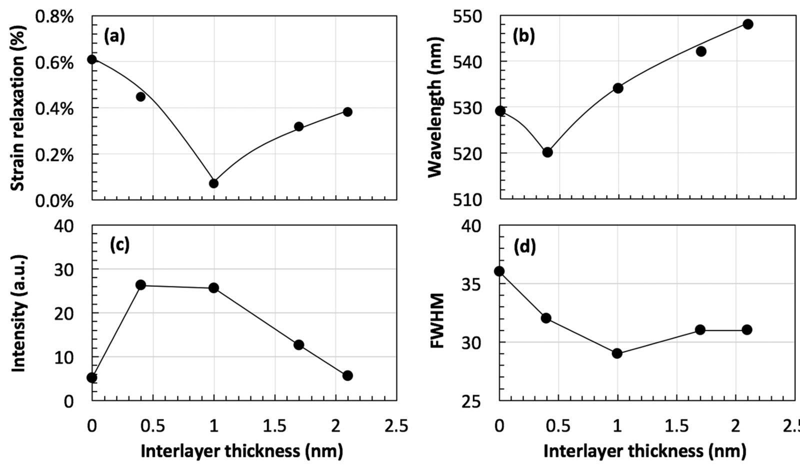

FIG. 4. Plot of a) relaxation percentage, b) peak photoluminescence wavelength, and c) photoluminescence intensity, and d) full-width-half-maximum (FWHM) versus interlayer thickness for the InGaN/AlGaN/GaN multiple quantum wells. Nearly pseudomorphic growth is achieved with a 1 nm thick interlayer. The wavelength, PL intensity, and FWHM change with interlayer thickness. The lines are guides to the eye.

InGaN relaxation, while the MQW peaks above the GaN peak are shifted in the direction of AlGaN relaxation (data not shown). This could be an indication that the interlayer MQW has different lattice constants in the respective InGaN and AlGaN layers indicating a severe breaking of pseudomorphic growth that is occurring throughout the MQW. This severe strain relaxation is probably an indication that the total strain and thickness have reached a critical limit. Further work is required to determine the exact nature of this relaxation.

Using Eqn. 1 and the RSM data in Fig. 3, the relaxation for the MQWs with different IL thicknesses are calculated and shown in Fig. 4(a). For the MQW without an IL the relaxation is 0.61%, and the relaxation decreases to 0.45% with the 0.4 nm thick IL. The lowest relaxation occurs for the 1 nm thick IL at a relaxation of 0.07%, and this relaxation indicates nearly pseudomorphic growth of the MQW. Finally, the relaxation increases to 0.32% and 0.38% for the interlayers with thicknesses of 1.7 nm and 2.1 nm, respectively.

The peak photoluminescence (PL) wavelength versus IL thickness is shown in Fig 4(b). For the MQW without AlGaN IL, the peak wavelength is 529 nm. As an IL is introduced into the structure, changes in energy barrier height and spontaneous and piezoelectric polarization shift the wavelength. The interplay of the transition wavelength and the resulting optoelectronics properties for InGaN QWs with AlGaN tensile barriers or interlayer can be found in previous theoretical work.[23,27] When comparing MQWs with 0 nm and 0.4 nm thick ILs, a stronger quantum confinement effect from a higher energy barrier is present in the 0.4 nm thick IL, which in turn increases the energy of the electronic states that blue-shifts the PL wavelength. This is despite the fact that the 0.4 nm thick interlayer MQW has slightly more indium in the QW, and should result in a red-shift in wavelength if the barriers were the same. Beyond 0.4 nm thick AlGaN ILs, the polarization-induced charge separation dominates in these InGaN QWs. The charge and resulting electric fields tilt the energy bands that become greater with increased thickness, resulting in a lower transition energy that increasingly red-shifts the wavelength with increased thickness. Fig. 4(b) shows that for ILs with thicknesses greater than 0.4 nm, as the IL thickness is increased there is a red-shift in peak wavelength. It should be noted that some of the red-shift in wavelength with increased thickness, from 0.4 nm to 1 nm, is due to a slight increase in indium concentration (see Fig. 2).

Fig 4(c) shows the PL intensity and Fig 4(d) shows the full width at half maximum (FWHM) versus IL thickness of the MQW structures. Introducing a 0.4 nm thick IL into the MQW structure increases the PL intensity by ~5 times and the FWHM narrows despite the larger indium concentration in the 0.4 nm thick IL sample. This increase is consistent with the improved optical matrix element from the stronger quantum confinement as predicted in previous theoretical work.[27] Another potential reason for increased PL intensity is better surface morphology. Previous work has shown that an

AlGaN capping layer improves rms surface roughness and reduces pit density.[21,23,32] This is contrary to MQWs without ILs that exhibit decreases in efficiency and widening of emission with increased indium (green gap).[33–35]

When the IL thickness is increased to 1 nm, the PL intensity remains almost the same and the FWHM narrows further. Energy band calculations predict that the intensity should have dropped significantly due to the reduction of electron-hole wavefunction overlap caused by larger polarization induced electric fields. However, the intensity remains the same experimentally. This is because for the 1 nm sample the relaxation is much smaller, indicating pseudomorphic growth (Fig. 4(a)). As a result, defect formation and non-radiative recombination is reduced as supported by even lower FWHM, and lower non-radiative recombination compensates for the decrease in overlap and leads to a greater radiative efficiency. As the IL thickness is increased beyond 1 nm, the PL intensity drops quite sharply and the FWHM increases. This sharp drop in intensity is due to a decrease in electron-hole wavefunction overlap due to larger piezoelectric polarization induced electric fields, and also increased defect formation due to increased relaxation and wider FWHM as the ILs increase in thickness (Fig 4(a)).

Given the success of interlayer MQWs, a predictive model would be useful in order to design MQWs emitting at different wavelengths. One should expect that the IL thickness required to achieve pseudomorphic growth will change with Al composition in the AlGaN IL, and the indium concentration and thickness of the InGaN QW. To that end, the zero-stress model[36,37] is investigated to understand if it can match the experimental data. The zero-stress model predicts an $Al_{0.42}Ga_{0.58}N$ IL thickness of ~6.5 nm to compensate for a 3.3 nm thick $In_{0.205}Ga_{0.795}N$ QW. Experimentally it is found that pseudomorphic growth is achieved at an IL thickness of 1 nm, much thinner than the zero-stress model predicts. The discrepancy in the modeled and experimental data is because the zero-stress model does not take into account the lattice mismatch strain between the InGaN and AlGaN layers, and it also does not consider the critical thicknesses of the layers. Clearly, a more predictive model is necessary to account for the presented data. Incorporating critical thicknesses values into the calculations will account for the inevitable increase in strain as subsequent QWs are grown. Introducing the AlGaN IL, clearly lowers the total critical thickness requirement resulting in a greater total thickness the InGaN QWs can achieve before relaxing.

In conclusion, AlGaN IL capped InGaN/AlGaN/GaN MQWs are grown with different IL thicknesses to study strain compensation. Our results demonstrate that, for a certain InGaN composition and thickness, there is an optimum thickness and composition of the AlGaN IL that can compensate the compressive strain in the InGaN QW. This enables pseudomorphic growth of the entire MQW stack, which in turn drastically reduces defect formation and enhances the radiative efficiency.

The authors would like to acknowledge funding from glō-USA, US National Science Foundation (Awards # 1408051, 1505122, 1708227), and the Daniel E. '39 and Patricia M. Smith Endowed Chair Professorship Fund (N.T.). Sandia National Laboratories is a multimission laboratory managed and operated by National Technology and Engineering Solutions of Sandia LLC, a wholly owned subsidiary of Honeywell International Inc. for the U.S. Department of Energy's National Nuclear Security Administration under contract DE-NA0003525.

[1] Y. Narukawa, M. Ichikawa, D. Sanga, M. Sano, and T. Mukai, J. Phys. D. Appl. Phys. **43**, 354002-1 (2010).
[2] M. R. Krames, O. B. Shchekin, R. Mueller-Mach, G. O. Mueller, L. Zhou, G. Harbers, and M. G. Craford, IEEE/OSA J. Disp. Technol. **3**, 160 (2007).
[3] S. Lutgen, D. Dini, I. Pietzonka, S. Tautz, A. Breidenassel, A. Lell, A. Avramescu, C. Eichler, T. Lermer, J. Müller, G. Bruederl, A. Gomez, U. Strauss, W. G. Scheibenzuber, U. T. Schwarz, B. Pasenow, S. Koch, O. Opto, and S. Gmbh, Library (Lond). **7953**, 1 (2011).
[4] C. A. Hurni, A. David, M. J. Cich, R. I. Aldaz, B. Ellis, K. Huang, A. Tyagi, R. A. Delille, M. D. Craven, F. M. Steranka, and M. R. Krames, Appl. Phys. Lett. **106** (2015).
[5] Y.-K. Ee, R. A. Arif, N. Tansu, P. Kumnorkaew, and J. F. Gilchrist, Appl. Phys. Lett. **91** (2007).
[6] S. Nakamura, M. Senoh, N. Iwasa, and S. I. Nagahama, Jpn. J. Appl. Phys. **34**, L797 (1995).
[7] M. H. Crawford, IEEE J. Sel. Top. Quantum Electron. **15**, 1028 (2009).
[8] J. M. Phillips, M. E. Coltrin, M. H. Crawford, A. J. Fischer, M. R. Krames, R. Mueller-Mach, G. O. Mueller, Y. Ohno, L. E. S. Rohwer, J. A. Simmons, and J. Y. Tsao, Laser Photonics Rev. **1**, 307 (2007).
[9] F. Scholz, A. Sohmer, J. Off, V. Syganow, A. Dörnen, J. Seo Im, A. Hangleiter, and H. Lakner, Mater. Sci. Eng. B **50**, 238 (1997).

[10] D. D. Koleske, S. R. Lee, G. Thaler, M. H. Crawford, M. E. Coltrin, and K. C. Cross, Appl. Phys. Lett. **97** (2010).
[11] D. D. Koleske, S. R. Lee, M. H. Crawford, K. C. Cross, M. E. Coltrin, and J. M. Kempisty, J. Cryst. Growth **391**, 85 (2014).
[12] D. D. Koleske, A. E. Wickenden, R. L. Henry, and M. E. Twigg, J. Cryst. Growth **242**, 55 (2002).
[13] N. Okada, K. Tadatomo, K. Yamane, H. Mangyo, Y. Kobayashi, H. Ono, K. Ikenaga, Y. Yano, and K. Matsumoto, Jpn. J. Appl. Phys. **53** (2014).
[14] X. H. Wu, C. R. Elsass, A. Abare, M. MacK, S. Keller, P. M. Petroff, S. P. Denbaars, J. S. Speck, and S. J. Rosner, Appl. Phys. Lett. **72**, 692 (1998).
[15] A. M. Armstrong, M. H. Crawford, and D. D. Koleske, Appl. Phys. Express **7** (2014).
[16] D. Cherns, S. J. Henley, and F. A. Ponce, Appl. Phys. Lett. **78**, 2691 (2001).
[17] V. Fiorentini, F. Bernardini, F. Della Sala, A. Di Carlo, and P. Lugli, Phys. Rev. B **60**, 8849 (1999).
[18] R. A. Arif, Y. K. Ee, and N. Tansu, Appl. Phys. Lett. **91**, 1 (2007).
[19] H. Zhao, G. Liu, J. Zhang, J. D. Poplawsky, V. Dierolf, and N. Tansu, Opt. Express **19**, A991 (2011).
[20] S. Saito, R. Hashimoto, J. Hwang, and S. Nunoue, Appl. Phys. Express **6**, 111004 (2013).
[21] R. Hashimoto, J. Hwang, S. Saito, and S. Nunoue, Phys. Status Solidi Curr. Top. Solid State Phys. **11**, 628 (2014).
[22] J. Il Hwang, R. Hashimoto, S. Saito, and S. Nunoue, Appl. Phys. Express **7** (2014).
[23] D. D. Koleske, A. J. Fischer, B. N. Bryant, P. G. Kotula, and J. J. Wierer, J. Cryst. Growth **415**, 57 (2015).
[24] J. P. Ahl, J. Hertkorn, H. Koch, B. Galler, B. Michel, M. Binder, and B. Holländer, J. Cryst. Growth **398**, 33 (2014).
[25] S. M. Myers and C. H. Seager, J. Appl. Phys. **95**, 520 (2004).
[26] K. Lekhal, B. Damilano, H. T. Ngo, D. Rosales, P. De Mierry, S. Hussain, P. Vennégués, and B. Gil, Appl. Phys. Lett. **106**, 142101 (2015).
[27] H. Zhao, R. A. Arif, Y. K. Ee, and N. Tansu, IEEE J. Quantum Electron. **45**, 66 (2009).
[28] N. Tansu and L. J. Mawst, IEEE Photonics Technol. Lett. **14**, 444 (2002).
[29] N. Tansu and L. J. Mawst, IEEE Photonics Technol. Lett. **13**, 179 (2001).
[30] S. Hussain, K. Lekhal, H. Kim-Chauveau, P. De Mierry, B. Damilano, and P. Venn, Semicond. Sci. Technol. **29**, 35016 (2014).
[31] J. J. Wierer, D. D. Koleske, and S. R. Lee, Appl. Phys. Lett. **100** (2012).
[32] R. Hashimoto, J. Hwang, S. Saito, and S. Nunoue, Phys. Status Solidi Curr. Top. Solid State Phys. **10**, 1529 (2013).
[33] T. Mukai, H. Narimatsu, and S. Nakamura, Japanese J. Appl. Physics, Part 2 Lett. **37** (1998).
[34] S. Yamamoto, Y. Zhao, C. C. Pan, R. B. Chung, K. Fujito, J. Sonoda, S. P. DenBaars, and S. Nakamura, Appl. Phys. Express **3** (2010).
[35] H. Sato, R. B. Chung, H. Hirasawa, N. Fellows, H. Masui, F. Wu, M. Saito, K. Fujito, J. S. Speck, S. P. DenBaars, and S. Nakamura, Appl. Phys. Lett. **92**, 221110 (2008).
[36] P. Harrison and A. Valavanis, Quantum Wells, Wires and Dots (2016).
[37] A. F. Wright, J. Appl. Phys. **82**, 2833 (1997).